Eleventh International Conference on the Bearing Capacity of Roads, Railways and Airfields, Volume 2 – Hoff, Mork & Saba (eds)

Freeze-thaw influence on the water retention capacity of silty sand subgrades

J.H.C Everton & D. Saliko
Division of Building Materials, ABE/BYV, Royal Institute of Technology/KTH, Stockholm, Sweden
Pavement Technology, Swedish National Road and Transport Research Institute - VTI, Linköping, Sweden

S. Erlingsson
Division of Building Materials, ABE/BYV, Royal Institute of Technology/KTH, Stockholm, Sweden
Pavement Technology, Swedish National Road and Transport Research Institute - VTI, Linköping, Sweden
Faculty of Civil Engineering and Environmental Engineering, University of Iceland, Reykjavik, Iceland

ABSTRACT: Fine-grained materials are associated with a higher water retention capacity due to their higher surface energy in comparison with coarser materials. That characteristic is connected to why fine-grained materials also yields more suction when drying. In addition, seasonal variation of the water table subjects fine-grained subgrades to different moisture contents, varying the suction built in the subgrade, consequently affecting its mechanical characteristics. As fine-grained materials are frequently frost susceptible, they can cause issues to the whole pavement cross-section related to Freeze-Thaw (F-T) actions, widely known as frost heave and thaw weakening. This study will seek to investigate if subsequent cycles of closed-system F-T can permanently alter the unsaturated behaviour of fine-grained materials, using as background their Soil Water Retention Capacity obtained using a pressure plate apparatus. Such issues may become more common with permafrost areas being subjected to freeze and thaw cycles due to climate change or extraordinary events creating the circumstances to F-T where it is currently not observed. Two silty sands with low plasticity were tested, and the results show a reduced water retention capacity (WRC) after closed-system F-T cycles. Considering that matric suction changes the state of stress of soils, the findings suggest an impact in the resilient modulus (M_r) not only seasonally, as it is well established, but also after seasonal freezing and thaw events.

Keywords: Swrc, unsaturated soils, subgrade, cold regions pavement structures, freeze-thaw

1 INTRODUCTION

Subgrades in frost susceptible regions follow the same principia as in non-frost susceptible regions regarding water protection. Such that one of the purposes of the pavement structure resting on top of the subgrade is to protect it from water infiltration; the other functions are to protect it from high vertical and shear stresses. Therefore, considering the lower permeability of the surface layer, one can say that the subgrades in frost regions are also situated in the intermediate vadose zone, where a two-phase of continuous water and air coexist, at least for parts of the year.

An important contrast, however, from non-frost-susceptible regions is the formation of ice lenses (depending on the frost susceptibility of the soil) during the winter, in a process known as ice segregation, where water is drawn up to the freezing front due to a cryosuction effect.

DOI: 10.1201/9781003222897-10

Then, this water in excess thaws and saturate the soil during the spring until it gradually dissipates, depending on the soil's permeability and external conditions.

Whereas in non-frost-susceptible regions, the mechanism of energy dissipation allows for evapotranspiration (Doré and Zubeck, 2009), which means the moisture content stabilises, reaching a steady-state condition (Zapata, 2018), where the subgrades will be mainly in the unsaturated condition, for most of the year unless during raining events where water can reach the pavement structure transversally, or axially, in case the surface has aged and cracks have developed.

Due to the high surface energy and swelling-prone property of fine-grained materials, unfrozen water bounded to the grains – known as adsorbed water – is observed even when temperatures are well below the freezing point (Andersland & Ladanyi, 2004), which means the ice crystals grown bigger within the pores until the adsorbed water freezes, potentially displacing the grains. In the spring, the unfrozen water saturates the subgrade, causing what is known as thaw weakening – reducing the pavement's bearing capacity. The literature and experience show that the bearing capacity of such pavements slowly returns to previous levels when the water is drained. In other words, suction will increase as water drains, increasing the mechanical characteristics of the subgrade.

However, some studies suggest that F-T cycles can cause particles to break up, changing the particle size distribution, which coupled with the ice expansion, that can cause a void ratio's increase or pore geometry change, can affect the Soil Water Retention Capacity (SWRC) of the subgrades (Ren & Vanapalli, 2019; Yao et al., 2020).

1.1 *Subgrades soils in frost regions*

Natural materials used as subgrade can suffer excessive permanent deformation if not adequately protected from high stresses and water infiltration. Consequently, it can fail to provide the necessary support for the asphalt layer, with shear stresses causing strains that exceed the fatigue resistance of such layer, resulting in cracking.

In cold regions, however, another challenge is added to protecting the subgrade, which is related to frost problems. To provide adequate protection to the subgrade, one design option is to have a thicker pavement structure to isolate or minimise the subgrade's exposure to the freezing front and its consequences, as explained before. The freezing index (FI) of the region, type of subgrade material, and natural water content are variables that will affect the frost depth ($\bar{x}$), that is, the depth the frost penetrates the ground during the winter season. There is more than one model to equate the frost depth, but Stefan Solution (Eq. 1) gives a good estimation, and the parameters are relatively simple to obtain. It relates the freezing index, the latent heat of fusion (L) and the heat conductivity (k_f), both of which are a function of the material and the water content (Andersland and Ladanyi, 2004).

$$\bar{x} = \sqrt{\frac{2k_f}{L} \cdot FI} \tag{1}$$

Other strategies to prevent frost problems include changing the subgrade material to one less susceptible to frost and, alternatively, providing drainage layers to remove water from the system so that it is not attracted to the freezing fringe. Nevertheless, the soil heterogeneity along a road section and different water contributors makes it hard to have full control of the freezing process within the subgrade, and so the pavement structure should resist some level of differential frost heave (Andersland and Ladanyi, 2004).

Another design method for cold region pavements accounts for a weakened subgrade when thawing during the spring (Andersland and Ladanyi, 2004). Thawing can occur even when no frost heaving occurs, which is related to the thawing speed and the material's permeability. An example of such an issue is clay, which combines high matric suction with low permeability, making the conditions for ice segregation difficult and, therefore, frost heave less severe. However, the entrapped water in a clay subgrade layer will significantly reduce the bearing capacity during thawing (Christopher et al., 2006).

In order to adequately estimate a pavement service life based on one of the design strategies mentioned above, we need to know the material's mechanical properties to verify if they can

sustain the stresses that will be yielded in the structure due to traffic and environmental conditions. In that regard, in a mechanistic-empirical (M-E) method, the strains of interest are the horizontal tensile strain at the bottom of the bounded layer and the vertical strain at the top of the subgrade to assess fatigue cracking and rutting, respectively. Finally, the layers corresponding to the pavement structure are evaluated in terms of their combined accumulated strain throughout the pavement design life against the backdrop of the maximum permissible rutting and fatigue cracking (Doré and Zubeck, 2009).

This research aims at contributing to the scholar on the M-E method by verifying the impact that freeze-thaw cycles have on the SWRC of subgrades and potentially in its mechanical characteristics. For that purpose, two silty sand subgrades with different fines content, from the region of Östergötland in Sweden, will have their SWRC determined.

2 CHARACTERISING UNSATURATED SUBGRADES

The so-called Soil Water Characteristic Curve (SWCC), which relates suction and moisture content, is a fundamental relationship to understanding the behaviour of unsaturated soils better. In fact, there is more than one curve describing the relationship of suction and moisture content for each soil, and it is conditioned to whether the soils are experiencing drying or wetting, to its initial dry density and its initial degree of saturation (Walshire et al., 2019). Therefore, some authors suggest calling such a relationship, obtained from one's experiment, as Soil Water Retention Capacity (SWRC) as it was originated with a particular set of boundary conditions.

Authors have identified that soils show a hysteresis behaviour when drying and wetting; that is, the relationship between suction and water content is different if the soil starts fully saturated or from a dry state. Those curves are known as main drying and main wetting curve. Previous research has shown that the obtained relationship would fit within the main curves for tests initiated from fully saturated to fully dry (residual saturation) (Fredlund et al., 2012).

The SWRC can be used to estimate unsaturated soil property functions (USPF), e.g. permeability, shear strength and volume change. Although those are empirical relationships, the results show a good fit with tests specifically designed to test those properties (Fredlund et al., 2012). The estimation of USPFs are related to the drying branch of the SWRC (Fredlund et al., 2012), coupled to that, most previous studies focused on desorption tests. Therefore, for comparison and repeatability with previous studies, this study focused on the drying SWRC.

The initial dry density is another parameter for a SWRC, and for naturally occurring materials such as subgrades, they are usually at least mechanically stabilised, i.e., they are compacted to a maximum dry density at an optimum moisture content (OMC).

In this study, two silty sands were tested, and Table 1 presents the index properties obtained before the sample preparation for the suction experiments. According to the Unified Soil Classification System (USCS), both soils are classified as Silty Sand material (SM), and according to tests performed on the material with 39% fines (Kuttah, 2020), it has a plasticity index of less than 4%, resulting in low plasticity soil. The material with 17% fines was deemed nonplastic.

In light of this, the results of this study will be interpreted according to SWRC for incompressible soils, where the gravimetric SWRC (*w-SWRC*) can be converted into volumetric (*θ-SWRC*) and degree of saturation (*S-SWRC*) relationships without the need to obtain shrinking parameters (Fredlund, 2019).

Table 1. Index properties of the tested soils.

Soil Classification	Passing sieve 0,063mm (%)	Max. Dry unit weight (g/cm^3)	Optimum Moisture cont. (%)	Specific gravity (-)	Liq. Lim. LL (%)	Pl. lim. PL (%)	Pl. Index PI (%)
SM	17,40	1,902	8,7	2,65	-	-	-
SM	39,00	2,083	8,5	2,64	18[1]	14,30[1]	3,70[1]

[1] Results obtained from (Kuttah, 2020) from tests conducted in the same material.

Therefore, after establishing the boundary conditions, a SWRC to characterise unsaturated subgrades could be obtained in the laboratory.

2.1 *SWRC testing*

There are at least two well-described methods to measure the relationship between suction and moisture content, one artificially imposes a pressure in the specimen to force water out and is known as the axis translation technique; the other measures water tension in a specimen as it dries (Briaud, 2013; Fredlund et al., 2012). Their use will depend on the suction range of interest, the type of soil and the time frame available. The particle size distribution plays a significant role in the consolidation time between different pressure targets, i.e., the rate of water release from the soil for a given suction.

For the suction level experienced in subgrade soils, a pressure plate apparatus, which employs the axis translation technique, suffices the requirements considerably faster when compared with the filter paper, which employs the other method described above. This research was conducted using a pressure plate apparatus, namely SWC-150 Fredlund SWCC Device (*Figure 1*). This apparatus can apply and sustain up to 1500 kPa of air pressure in a cell chamber, and the consolidation time between applied pressures vary from several hours to days, whilst the filter paper varies from two to five days (Erlingsson et al., 2009).

Matric suction (ψ) is emulated using the SWC-150 by increasing the pore air pressure (u_a) while keeping the pore water (u_ω) at atmospheric pressure. For in situ conditions, matric suction is yielded with negative water pressures while the air pressure is kept at atmospheric level; the outcome is that the same matric suction from the field can be yielded in the laboratory (2). Furthermore, field conditions are attained in metastable conditions, where water can remain in liquid state even with negative pressure; however, if such conditions were applied in the laboratory, a cavitation process would occur, and water readings would not be meaningful (Marinho et al., 2008). Therefore, in the axis translation technique, the air pressure is intentionally higher than the atmospheric pressure to fall into a stable condition (*Figure 2*), controlling the formation of bubbles in the water reservoir below the ceramic stone seen in *Figure* 1a.

$$\psi = (u_a - u_w)_{in\ situ} = (u_a - u_w)_{axis\ translation} \tag{2}$$

Figure 1. SWC-150 Device. a) Bottom plate with the HAE ceramic stone installed into its recess b) specimen mounted on top of the ceramic stone and chamber cell positioned c) enclosed pressure chamber with top plate.

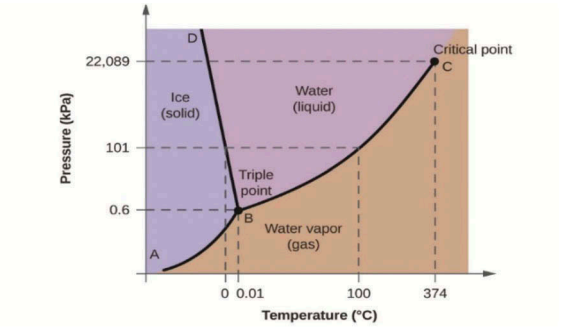

Figure 2. The phase diagram of water under stable conditions (licensed under CC BY).

2.2 *Testing preparation*

In the SWC-150 device, a metal ring is used as a sample holder, and it has a height of 32mm and 51mm in diameter. The samples were compacted to modified Proctor energy (2,7 MJ/m^3) using a rammer compactor seen in *Figure 3a* (Walshire et al., 2019).

A total of 4 samples (*Figure 3b*) for each soil were prepared at OMC and, using the same compaction effort, sealed with plastic foil to retain moisture and later subjected to cycles of freeze and thaw. *Figure 3c* shows one of the two batches with samples identified from 0 to 5 F-T cycles of 48h for each cycle (24h Freezing at -20 °C and 24h thawing at +20 °C). These temperatures and time-span were calculated in order to completely freeze and thaw the water within the sample, aiming at creating an accelerated F-T process and they find resonance in recently published papers (Ding et al., 2020; Ren & Vanapalli, 2019; Yao et al., 2020).

The method used to subject the samples to F-T is known as closed-system and it differs from an open-system, as in the latter, the sample has access to a water source throughout the freezing process. The closed-system method with three-dimensional freezing was adopted due to the practicality it offers in comparison with an open-system with uniaxial freezing imposition, which would require a distinct experimental setup. The issue revolves about preparing a smaller recompacted sample, suitable to be tested in the SWC apparatus, and yet providing access to a water source while imposing freezing uniaxially during F-T cycles.

Even though the closed-system could be seen as a simplification from field conditions, for soils with lower permeability (as low as a $k \ll 1x10^{-7} cm/s$), the frost penetration rate is often greater than the rate in which water reaches the freezing front, thus having access to water would be indifferent in this case, as the water source would freeze as well and the moisture movement to the freezing front would be restricted (see Wong & Haug, 1991). Furthermore, as material heterogeneity is expected in naturally occurring materials as subgrades, both closed-system and open-system can be seen as representations that may be expected to a certain extent in the field (Wong & Haug, 1991).

Hence, due to the nature of materials used in this study and the sampling setup, a closed-system with triaxial F-T was considered adequate to acquire a better understanding of possible effects of F-T to material's properties.

Before being tested in the SWC device, as shown in *Figure 1,* the samples were saturated at least overnight after being subjected to closed-system F-T cycles. A sample is shown in *Figure 3d*, where it is resting on top of a porous stone to regulate the flow of water and with a filter paper separating them to avoid material loss. The SWRC was determined as per ASTM D6836-16 (ASTM, 2016).

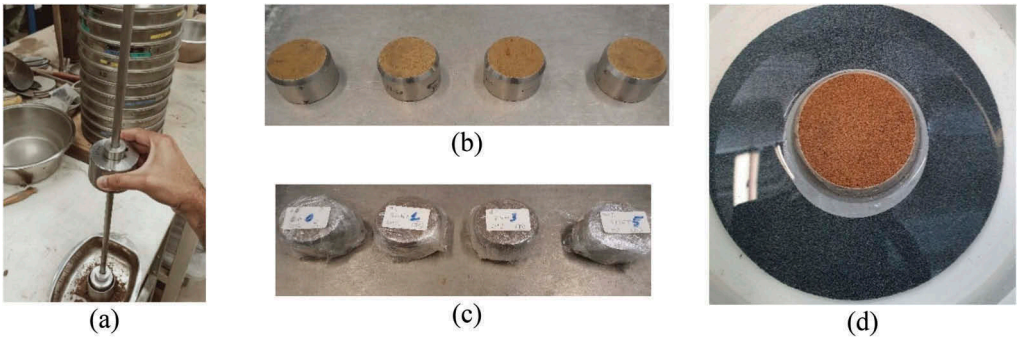

Figure 3. Sample preparation. a) Rammer compactor for small samples b) compacted samples at maximum optimum content c) conditioned samples for freeze and thaw cycles, from 0 to 5 cycles (NFT0 to NFT5) d) saturation process, before the sample is subjected to desorption in the SWC-150.

2.3 *SWRC modelling*

There are many available models to fit experimental data into continuous functions to describe the suction and water content relationship. Two of the most used ones were used in this study: the Van Genuchten 1980 (4) and the Fredlund and Xing 1994 (5). A third equation is presented by Brooks and Corey 1964 (3) and it was tested due to its ability to represent sharp air entry values (McCartney, 2007), observed in the SM with 17% fines.

$$\text{Brooks and Corey (1964)}\ \theta(\psi) = \theta_r + (\theta_s - \theta_r).(\psi/\psi_{AEV})^{-\lambda_{BC}} \tag{3}$$

$$\text{Van Genuchten (1980)}\ \theta(\psi) = \theta_r + (\theta_s - \theta_r).\left[1 + (\alpha.\psi)^N\right]^{-\left(1-\frac{1}{N}\right)} \tag{4}$$

$$\text{Fredlung Xing (1994)}\ \theta(\psi) = C(\psi).\left\{\theta_s/\left[ln\left(e + (\psi/a_f)^{n_f}\right]^{m_f}\right\}\right. \tag{5}$$

$$C(\psi) = 1 - ln[1 + (\psi/\psi_r)]/ln\left[1 + \left(10^6/\psi_r\right)\right] \tag{6}$$

Where for Brooks and Corey, ψ is the matric suction, θ_s is the saturated volumetric water content, θ_r is the residual volumetric water content, and λ_{BC} is a fitting parameter. For the Van Genuchten model, the first part is similar to the previous model, but instead of a power-law function, a hyperbolic function is introduced, where α is related to the inverse of the Air Entry Value (AEV) and N is a dimensionless fitting parameter. Finally, for Fredlund and Xing model, a_f is related to the AEV, n_f is related to the pore-size distribution (McCartney, 2007) and is a rate of desorption after the AEV (Zapata, 2018), whereas m_f is related to the residual water content (Zapata, 2018) and represents the model skew (McCartney, 2007).

Statistical analysis was used to assess the model fits of the data. The analysis was based on the sum of squares of errors (SSE) resulting from the difference between the measured and curve fitted results. Table 2 shows that Fredlund and Xing demonstrate good agreement with the measured data, except for one of the tests, which Van Genuchten described better (NFT5). It is worth mentioning that the correlation coefficient (R^2) shows a strong relationship between the model parameters and the calculated result for all models. For comparison and repeatability, the Fredlund and Xing 1994 model was adopted to perform the subsequent analysis.

Table 2. Curve fitting statistics for the silty sand with 17% fines.

	NFT0		NFT1		NFT3		NFT5	
Model	SSE	R^2	SSE	R^2	SSE	R^2	SSE	R^2
Fredlund & Xing	**1,968**	**0,996**	**1,827**	**0,997**	**0,767**	**0,999**	5,790	0,989
Van Genuchten	35,928	0,930	32,120	0,944	25,203	0,955	**4,495**	**0,992**
Brooks & Corey	43,651	0,890	36,498	0,922	46,561	0,899	35,520	0,916

3 ANALYSIS AND DICUSSION

Tests in the SM material with 17% fines (*Figure 4*) showed that the AEV was not particularly influenced by the F-T cycles, with the a_f ranging from 7,16 kPa for 0 F-T to 6,91 kPa for 5 F-T; but increasing and decreasing in the interval. On the other hand, the rate of desorption once the AEV was reached, n_f, changed significantly, decreasing from 36,53 to 9,75 in the same comparison. The fitting parameter m_f increased from 0,18 to 0,41 and it can be seen that it is proportionally inverse to the residual water content. Thus, the higher the m_f, the lower the residual water content. Finally, the residual suction decreased from 80 kPa to 30 kPa in 5 cycles of F-T. These results suggest some shift in the unsaturated behaviour of this material, where the same water content yielded less suction with the increase of the number of F-T cycles.

Figure 5 presents the results for the material with 39% fines. The a_f results suggest an increasing trend in the AEV, ranging from 12,95 kPa to 15,07 kPa from 0 to 5 F-T cycles, respectively. The desorption rate n_f increased from 4,51 to 25,50, and the residual water parameter m_f ranged from 0,21 to 0,19; whereas the residual suction decreased from 750 kPa to 150 kPa in 5 F-T cycles. A similar conclusion can be made in comparison to the other soil, that less suction is yielded with the same water content as F-T cycles increases, although the results show a sharper contrast from the first cycle of F-T, in line with previous studies.

The increased AEV may find resonance in the frost penetration theory depicted in Stefan solution (1), where the frost depth increases with falling air temperatures during winter, meaning the pore water starts to freeze from closer to the surface downwards, consequently reducing the availability of unfrozen water. One of the effects is an overall reduction in pore size, which increases the AEV (Noh et al., 2012); and the other is that the menisci between pore water and grain particles are more tensioned, yielding more suction and possibly attracting more water to the freezing front.

Such effect could change the balance in the vadose zone, shown in *Figure 6*, and the water in the capillary fringe – corresponding to the region below the AEV – could be pulled upwards. In other words, ψ_{AEV} can be different among unfrozen and frozen soils of the same type, bulk density and initial water content (Noh et al., 2012; Ren and Vanapalli, 2019).

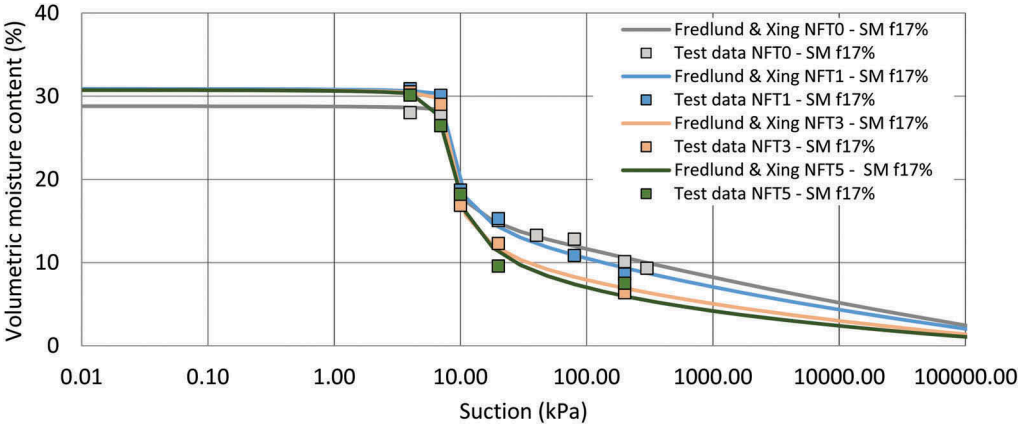

Figure 4. SWRC for silty sand with 17% fines, compacted to 95% modified Proctor energy.

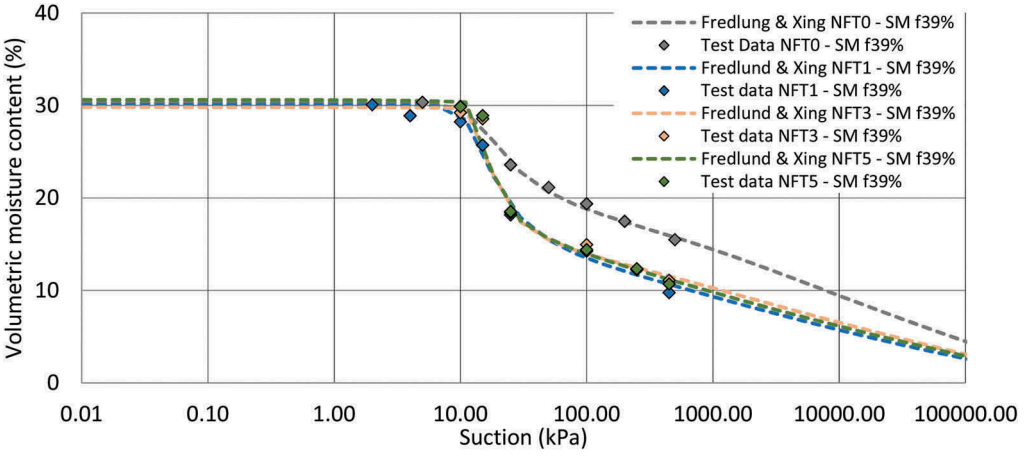

Figure 5. SWRC for a silty sand with 40% fines, compacted to 95% modified Proctor energy.

Table 3. Model parameters using Fredlund & Xing SWCC curve fitting model.

F-T cycles | soil	ψ_r (kPa)	a_f (kPa)	n_f (-)	m_f (-)	SSE (-)	R^2 (-)
0 F-T | SM *f=17%*	80	7,16	36,53	0,18	1,97	0,996
1 F-T | SM *f=17%*	47	7,42	25,90	0,23	1,83	0,997
3 F-T | SM *f=17%*	47	7,29	19,10	0,32	0,77	0,999
5 F-T | SM *f=17%*	30	6,91	9,75	0,41	5,79	0,989
0 F-T | SM *f=39%*	750	12,95	4,51	0,21	0,83	0,996
1 F-T | SM *f=39%*	450	12,18	5,76	0,31	5,32	0,990
3 F-T | SM *f=39%*	350	15,16	22,67	0,19	1,51	0,996
5 F-T | SM *f=39%*	150	15,07	25,50	0,19	0,75	0,998

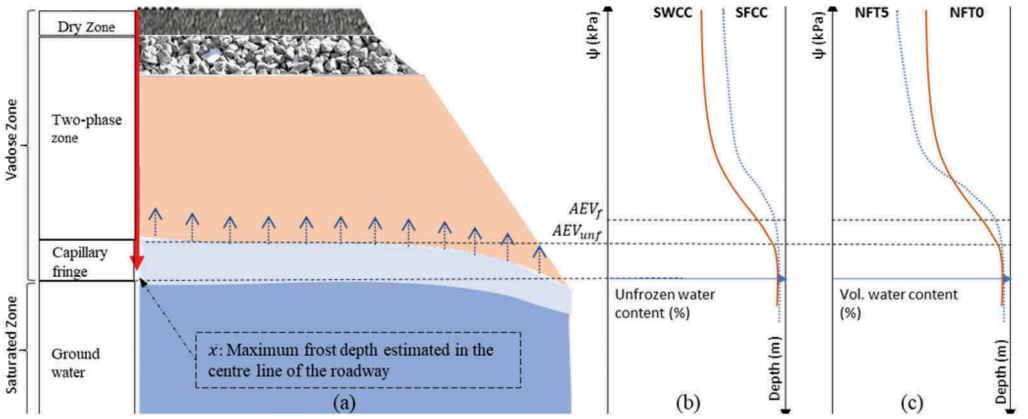

Figure 6. A) Vadose zone below a pavement structure b) idealised suction and unfrozen water content relationship from cryo-SWCC and SFCC studies c) idealised SWRCs representing data compiled in the present study.

Cryo-SWCC (Noh et al., 2012) and Soil-Freezing Characteristic Curve (SFCC) (Ren and Vanapalli, 2019) studies suggest the increase in AEV (*Figure 6b)* when comparing a single thawing sample with an unfrozen sample, but no permanent change is discussed. In the current study, SWRC model parameters were obtained from samples tested at room temperature after being subjected to F-T cycles, and they show a trend for WRC reduction. *Figure 6c* shows idealised SWRCs based on the data compiled in the study, and they differ from *Figure 6b* in the sense that they suggest a permanent shift in the SWRC post F-T cycles.

4 CONCLUSION

The studies on F-T of subgrades are needed to better understand the impacts on their mechanical characteristics. The results from the current study are limited to two silty sands with low plasticity; and the results conclude that 1) there is a reduction in WRC with increasing number of F-T cycles; 2) the contrast between the null sample (NFT0) and the other is higher with increased fines content.

More pronounced results would be expected if the samples had access to water during the cycles of freeze and thaw because then the freezing and thawing would be coupled with drying and wetting cycles. In addition, if freezing were imposed uniaxially, it would generally cause water movement to the freezing front, which creates a non-uniform degree of compaction within a sample (Wong and Haug, 1991). However, as this study was conducted imposing freezing triaxially, it is not expected significant water movement, thus no ice segregation, but rather ice crystals formation within particle's pores.

Other than its own properties, as the SWRC, a subgrade will likely be affected by F-T cycles by different degrees according to the layers' thicknesses above it and their thermal conductivity, not to mention water availability within the system. It is out of the scope of the present study to verify all those implications. It does, however, exemplify that there are many nuances for how freezing is imposed in the field, and in the present study, given the sample's size (32mm), triaxial freezing was considered adequate.

Previous studies suggest that the effects of F-T cycles stabilise between 6 and 7 cycles, but due to time constraints, the number of samples was limited. In future studies, it will be aimed to increase the number of samples to verify such stabilisation effect. Furthermore, the present study established a difference in how much suction is yielded in samples with the same water content for a different number of F-T cycles, and as suction changes the stress state of the soil, it impacts the resilient modulus (Doré and Zubeck, 2009). The result from the current study merits a further investigation to assess the extension of the impact in the Mr. including a setup to allow uniaxial freezing and thawing of samples in an open-system.

ACKNOWLEDGMENT

This work was sponsored by the Swedish Transport Administration (Trafikverket).

REFERENCES

Andersland, O. B., & Ladanyi, B. (2004). *Frozen ground engineering* (2nd ed). Wiley;ASCE.

ASTM. (2016). *Test Methods for Determination of the Soil Water Characteristic Curve for Desorption Using Hanging Column, Pressure Extractor, Chilled Mirror Hygrometer, or Centrifuge* (No. D6836-16). ASTM International. https://doi.org/10.1520/D6836-16

Briaud, J.-L. (2013). *Geotechnical Engineering: Unsaturated and Saturated Soils*. Somerset: John Wiley & Sons, Incorporated.

Christopher, B. R., Schwartz, C., & Boudreau, R. (2006). *Geotechnical aspects of pavements*. FHWA. https://www.fhwa.dot.gov/engineering/geotech/pubs/05037/

Ding, L., Han, Z., Zou, W., & Wang, X. (2020). Characterizing hydro-mechanical behaviours of compacted subgrade soils considering effects of freeze-thaw cycles. *Transportation Geotechnics*, *24*, 100392. https://doi.org/10.1016/j.trgeo.2020.100392

Doré, G., & Zubeck, H. K. (2009). *Cold regions pavement engineering*. ASCE Press;McGraw-Hill.
Erlingsson, S., Baltzer, S., Baena, J., & Bjarnason, G. (2009). Measurement techniques for water flow. In A. Dawson (Ed.), *Water in road structures* (pp. 45–67). Springer.
Fredlund, D. G. (2019). State of practice for use of the soil-water characteristic curve (SWCC) in geotechnical engineering. *Canadian Geotechnical Journal*, *56*(8), 1059–1069. https://doi.org/10.1139/cgj-2018-0434
Fredlund, D. G., Rahardjo, H., & Fredlund, M. D. (2012). *Unsaturated soil mechanics in engineering practice*. John Wiley & Sons, Inc.
Kuttah, D. (2020). *Development of a simple field method for measuring permanent deformations in silty sand subgrade* (VTI rapport 1086A; p. 46). VTI. http://vti.diva-portal.org/smash/record.jsf?pid=diva2%3A1557654&dswid=6775
Marinho, F. A. M., Take, W. A., & Tarantino, A. (2008). Measurement of Matric Suction Using Tensiometric and Axis Translation Techniques. *Geotechnical and Geological Engineering*, *26*(6), 615–631. https://doi.org/10.1007/s10706-008-9201-8
McCartney, J. S. (2007). *Determination of the hydraulic characteristics of unsaturated soils using a centrifuge permeameter* [PhD Thesis, The University of Texas at Austin]. http://citeseerx.ist.psu.edu/viewdoc/download?doi=10.1.1.822.6593&rep=rep1&type=pdf
Noh, J.-H., Lee, S.-R., & Park, H. (2012). Prediction of Cryo-SWCC during Freezing Based on Pore-Size Distribution. *International Journal of Geomechanics*, *12*(4), 428–438. https://doi.org/10.1061/(ASCE)GM.1943-5622.0000134
Ren, J., & Vanapalli, S. K. (2019). Comparison of Soil-Freezing and Soil-Water Characteristic Curves of Two Canadian Soils. *Vadose Zone Journal*, *18*(1), 1–14. https://doi.org/10.2136/vzj2018.10.0185
Walshire, L., Taylor, O.-D., & Berry, W. (2019). *Laboratory measure of SWCC for a poorly graded fine sand*. Engineer Research and Development Center (U.S.). https://doi.org/10.21079/11681/33676
Wong, L. C., & Haug, M. D. (1991). Cyclical closed-system freeze–thaw permeability testing of soil liner and cover materials. *Canadian Geotechnical Journal*, *28*(6), 784–793. https://doi.org/10.1139/t91-095
Yao, Y., Luo, S., Qian, J., Li, J., & Xiao, H. (2020). Soil-Water Characteristics of the Low Liquid Limit Silt considering Compaction and Freeze-Thaw Action. *Advances in Civil Engineering*, *2020*, 1–13. https://doi.org/10.1155/2020/8823666
Zapata, C. E. (2018). Empirical Approach for the Use of Unsaturated Soil Mechanics in Pavement Design. *PanAm Unsaturated Soils 2017*, 149–173. https://doi.org/10.1061/9780784481677.008